Nonlinear observer based fault detection and isolation for a momentum wheel

Jensen, Hans-Christian Becker; Wisniewski, Rafal

Publication date:
2001

Document Version
Også kaldet Forlagets PDF

NONLINEAR OBSERVER BASED FAULT DETECTION AND ISOLATION FOR A MOMENTUM WHEEL

Hans-Christian B. Jensen, Rafał Wiśniewski

Department of Control Engineering, Institute of Electronic Systems, Aalborg University
9220 Aalborg Ø, Denmark, Phone: 45 96358700, Fax: 45 98151739
Email: hcbj@control.auc.dk, raf@control.auc.dk

Abstract

This article realizes nonlinear Fault Detection and Isolation for a momentum wheel. The Fault Detection and Isolation is based on a Failure Mode and Effect Analysis, which states which faults might occur and can be detected. The algorithms presented in this paper are based on a geometric approach to achieve nonlinear Fault Detection and Isolation. The proposed algorithms are tested in a simulation study and the pros and cons of the algorithm are discussed.

1. INTRODUCTION

The stress on a new generation of spacecraft is on reducing the overall cost of a mission. This can be done be decreasing the size and complexity of the spacecraft and/or increasing the on-board autonomy. An autonomous spacecraft shall reduce the interaction with the ground-station's personal to the absolute minimum.

A significant part of the development of the on-board autonomy is an issue of making the spacecraft tolerant towards these faults, which can jeopardise the whole mission. In this article the focus is on momentum wheels. The model for the momentum wheel is based on the digital momentum/reaction wheel of the model TELDIX "ASSY RSI 01-5" for small and low-cost spacecraft and the momentum wheel for the Rømer satellite.

This article will contain a FMEA (Failure Mode and Effect Analysis) and geometric FDI (Fault Detection and Isolation) algorithms for the presented momentum wheel.

The first part of the paper is devoted to the possible faults occurring in a momentum wheel are identified. The faults are identified using FMEA. The third section contains a an overview of the geometric approach to FDI. In the fourth section nonlinear FDI algorithms are developed for isolating and detecting the faults described in the second section. The algorithms are then validated in a simulation study. Finally in the last section, the geometric method for deriving nonlinear FDI algorithms are discussed.

2. FMEA FOR A MOMENTUM WHEEL

This analysis helps to generate the proper residuals used for FDI. It also reveals which faults are observable/detectable.

The first part of FMEA is the failure causes. The failure causes for a momentum wheel are: Wear/tear (Usage/Radiation), transport to launch site, a too large acceleration during launch and too high or low power. The severity class of the failures depends on the number of momentum wheels on the spacecraft.

Table 1. Severity class [1] of failures and causes.

Function	Item	Number of Momentum Wheels on the spacecraft	Severity Class of Failure		
			1 Fails	2 Fails	3 Fails
Actuators	Momentum Wheel	4	III	II	I
Actuators	Momentum Wheel	3	II	I	I

Table 2. Faults in Momentum Wheel (MW) caused by outside components and faults in the motor.

Item	Failure Modes	Failure Effects		
		Local Effects	Next Level Effects	End Effects
MW	Loss of Power (100 %)	MW stops	No control momentum from this MW	Slower slew
MW	Loss of Power (Brown out)	Watchdog detects and stops MW	No control momentum from this MW	Slower slew
MW motor (bearing)	Mechanical breakage	Friction increases until rotor stops	No control momentum from this MW	Slower slew
MW motor (bearing)	Overheating/Mechanical breakage	Friction increases periodic/constant	Less control momentum	Slower slew and jitter in attitude
MW motor (Shaft or coupling)	Mechanical breakage (Shaft break)	Wheel stops	No control momentum from this MW	Slower slew
MW motor (Shaft or coupling)	Loose connection (Coupling break)	More heat generated and slower wheel spin	Less control momentum	Slower slew and jitter in attitude
MW motor (Stator Windings)	Overheating	Resistance in stator and heat increases	Longer reaction time	Higher power usage
MW motor (Stator Windings)	Overheating/Mechanical breakage	One of the windings is disconnected	Loss of motor effi -ciency and torque	Slower slew and jitter in attitude
MW motor (Stator Windings)	Insulation breakdown	Lower resistance in stator	Less control momentum	Slower slew and jitter in attitude
MW motor (Stator Windings)	Insulation breakdown	One of the windings short circuit	Loss of motor effi -ciency and torque	Slower slew and jitter in attitude and damage to electronics
MW motor (Stator Windings)	Electrical fault or malfunction	Periodic/constant short circuit	Loss of motor effi -ciency and torque	Slower slew and jitter in attitude and damage to electronics
MW motor (Stator Windings)	Electrical fault or malfunction	Periodic/constant disconnect	Loss of motor effi -ciency and torque	Slower slew and jitter in attitude
MW motor (Rotor bars or rings)	Mechanical breakage	Overheating /Vibrations /Torque pulsations/ Speed fluctuations/ current increase in remaining bars	Loss of motor effi -ciency and torque	Slower slew and jitter in attitude and further damage to remaining bars

Table 3. Faults in the control logic in a Momentum Wheel (MW).

Item	Failure Modes	Failure Effects		
		Local Effects	Next Level Effects	End Effects
MW Communication (RS485)	Disconnected (Both ways)	MW keeps present speed/ACS told nothing	Constant control momentum from this MW	Slower slew and problems with the estimator
MW Communication (RS485)	Disconnected (No Receive)	MW keeps present speed	Constant control momentum from this MW	Slower slew
MW Communication (RS485)	Disconnected (No Send)	MW works/ACS told nothing	Missing input to estimator	Problems with the estimator
MW EEProm	Bit value change, due to radiation	Reboot by Watchdog	No control momentum from this MW, during reboot	Slower slew during reboot
MW DSP	Dead lock	DSP stops working and is rebooted (Watchdog)	No control momentum from this MW, during reboot	Slower slew during reboot
MW Sensors	If the majority fails	Wrong torque and input to MW controller and ACS	Unknown torque (Constant/periodic)	Slower slew, jitter in attitude and problems with the estimator
MW 3 Phase Power FET	Electrical fault or malfunction	Periodic/constant short circuit	Loss of motor effi -ciency and torque	Slower slew and jitter in attitude and damage to electronics
MW 3 Phase Power FET	Electrical fault or malfunction	Periodic/constant disconnect	Loss of motor effi -ciency and torque	Slower slew and jitter in attitude
MW Voltage Regulator	Wrong output voltage	MW stops (Watchdog)	No control momentum from this MW	Slower slew
MW Watchdog (FPGA)	Fails	Reboot of DSP and /or MW stops	No control momentum from this MW (Constant/Periodic)	Slower slew and jitter in attitude

From the FMEA it can be seen that all the faults can be divided into seven groups according to the fault propagation characteristics. All the groups except the one containing overheating in the stator windings can be isolated and detected. This fault/group could be detected if a current measurement was available.

3. GEOMETRIC FAULT DETECTION AND ISOLATION

The geometric observer based methods are in the very focus of this paper. The methods are based on the results developed for nonlinear control theory [2]. The ideas were adopted for the purpose of the FDI by [3].

The main idea of geometric FDI is to design an observer such that only one fault is visible, whereas all the other faults and the disturbances acting on the momentum wheel are invisible in the residual. In this way the disturbances and other faults have no effect on the residual and there are no wrong fault detections.

Geometry is useful in the design of FDI, since it is a good tool for defining un- and observable spaces of a dynamic control system. The way to use geometry in FDI is to first find the smallest distribution D_1 which contains all the disturbances (The unwanted faults in the residual are treated as disturbances). This is the space the geometric FDI algorithm should place in the unobservable space. The second step is to find the largest observable codistribution which does not contain the distribution D_1. This information is then used to make a coordinate transformation, so that the transformed system has at least one state which is effected by the isolated fault and is unaffected by unmeasurable/unpredictable disturbances and unwanted faults. These states are then used for the observer.

3.1. Unobservability Distribution Algorithm

The unobservability algorithm is described in [4]. The distribution $P = \text{span}\{p_1, \ldots, p_d\}$ is spanned by the set of additional smooth vector fields $p_1(x), \ldots, p_d(x)$. The nondecreasing sequence of distributions are defined as follows:

$$\begin{aligned} S_0 &= \bar{P} \\ S_{k+1} &= \bar{S}_k + \sum_{i=0}^{m} \left[g_i, \bar{S}_k \cap \text{Ker}\{\text{d}h\} \right], \end{aligned} \tag{1}$$

where $\bar{S}$ denotes the involutive closure [5] of S. Suppose there exists an integer k^* such that

$$S_{k^*+1} = \bar{S}_{k^*} \tag{2}$$

and the set $\sum_*^P = \bar{S}_{k^*}$. Then $\sum_*^P$ is involutive, contains P and is conditioned invariant [3]. Any distribution D_2 which is involutive, contains P and is conditioned invariant satisfies $\sum_*^P \subseteq D_2$. So $\sum_*^P$ is the minimal element (with respect to distribution inclusion) of the family of all involutive conditioned invariant distributions which contain P.

The stopping condition (2) holds for some $k^* \leq n-1$ if all distributions generated by the algorithm 1 are nonsingular. If $\sum_*^P$ is well-defined (i.e. condition 2 holds) and nonsingular, so that its annihilator is locally spanned by exact differentials (because it is by construction involutive), and if $\sum_*^P \cap \text{Ker}\{\text{d}h\}$ is a smooth distribution, then it can be asserted that $(\sum_*^P)^\perp$ is the maximal (in the sense of codistribution inclusion) conditioned invariant codistribution which is locally spanned by exact differentials and contained in $P^\perp$.

3.2. Observability Codistribution Algorithm

The observability codistribution algorithm is described in [6]. Let ω be a fixed codistribution and define nondecreasing sequence of codistributions (Observability Codistribution Algorithm):

$$\begin{aligned} Q_0 &= \omega \cap \text{span}\{\text{d}h\} \\ Q_{k+1} &= \omega \cap \left(\sum_{i=0}^{m} L_{g_i} Q_k + \text{span}\{\text{d}h\} \right) \end{aligned} \tag{3}$$

If all the codistributions are nonsingular, then this algorithm is to be continued until $Q_{k^*+1} = Q_{k^*}$ for an $k^* \leq n-1$. Use notation $\omega^* = oca(\omega)$ for $\omega^* = Q_{k^*}$. Note $\omega^* = oca(\omega^*)$, so $oca(\omega^*)$ is the maximal (in the sense of codistribution inclusion) observability codistribution contained in ω^*. With other words if ω is a conditioned invariant codistribution [3], then $oca(\omega)$ is an observability codistribution.

If $\sum_*^P$ is well-defined (i.e. condition 2 holds for some k^*) and nonsingular, and that $\sum_*^P \cap \text{Ker}\{\text{d}h\}$ is a smooth distribution. Then $oca((\sum_*^P)^\perp)$ is the maximal (in the sense of codistribution inclusion) observability codistribution which is locally spanned by exact differentials and contained in $P^\perp$.

3.3. Geometric FDI Design method

The design method consists of the following five steps:

1. Write system in such a way, that L spans the fault that is going to be isolated and P spans the remaining faults and disturbances.
2. Find the minimal element ($\sum_*^P$) of the family of all involutive conditioned invariant distributions which contain P. So $\sum_*^P$ spans the space that is effected by the disturbances and remaining faults.
3. Then find the maximal observability codistribution (Ω) contained in $(\sum_*^P)^\perp$. This is the observable space which is not effected by the disturbances and remaining faults.
4. The unobservable distribution (Δ) is equal with $\Omega^\perp$.
5. Then use this information to design an observer for the isolated fault. The observer design is based on the Luenberger observer design and is described in the next five points:
   (a) The new system has a ${}^{new}P \in \Delta$, ${}^{new}L \notin \Delta$ and state $z \in \Delta$.
   (b) Use $\Omega \cap \text{span}\{\text{d}h\} = \text{span}\{\text{d}(\Psi_1 \circ h)\}$ to calculate Ψ_1, where $\dim(h) = p$, $\dim(\Omega \cap \text{span}\{\text{d}h\}) = n_2$ and $\dim(\Psi_1) = (p - n_2) \times p$.
   (c) The selection matrix H_2 is a $n_2 \times p$ matrix, in which some $p - n_2$ columns are zero, while the others are columns of a $n_2 \times n_2$ identity matrix.
   (d) Use $\Omega = \text{span}\{\text{d}\psi_1\}$ to calculate ψ_1, where $\dim(\Omega) = n_1$ and $\dim(\psi_1) = n_1 \times n$.
   (e) Find a ψ_3 such that $\psi_3 : U^\circ \to \mathbb{R}^{n-n_1-n_2}$, where U° is a neighbourhood of x°.

Structure of simple observer and residual generation:

$$\dot{z} = f(y,z) + \sum_{i=1}^{m} g_i(y,z)u_i + K_{obs}(h(z) - y) \tag{4}$$

$$r = h(z) - y \tag{5}$$

4. FAULT DETECTION AND ISOLATION ALGORITHMS FOR A MOMENTUM WHEEL

Geometric FDI for a momentum wheel can not be done for the whole operation range of the momentum wheel, since the state space model of a momentum wheel (See eq. (6)) is not a smooth C^∞ manifold. The operation range can be divided into two open subsets which are smooth. These subsets range respectively from zero to maximum velocity in one direction and from zero to maximum velocity in the other direction. These ranges are also the best operating ranges, since zero is one of the most wearing operating points for the motor.

4.1. Actuator Fault

The model for a momentum wheel is based on the model of a motor, which can be derived from [7].

$${}^{w}\dot{\omega}_w = \frac{K_t}{R_s\ I_w} v_s - \frac{K_t\ K_e + B_v\ R_s}{R_s\ I_w} {}^{w}\omega_w - \frac{B_c}{I_w}\text{sign}({}^{w}\omega_w) + L\,{}^{w}\omega_{act,w} \tag{6}$$

The observer is derived according to the presented method. The observer:

$$\begin{aligned} {}^{w}\dot{\omega}_{obs,w} &= \frac{K_t}{R_s\ I_w} v_s - \frac{K_t\ K_e + B_v\ R_s}{R_s\ I_w} {}^{w}\omega_{obs,w} - \frac{B_c}{I_w}\text{sign}({}^{w}\omega_{obs,w}) \\ &\quad + K_{obs}({}^{w}\omega_w - {}^{w}\omega_{obs,w}) \\ r &= {}^{w}\omega_{obs,w} - {}^{w}\omega_w \end{aligned} \tag{7}$$

4.2. Actuator Fault and Predicted Disturbance

The model is based on eq. (6), where the predicted disturbance is added to the system.

$$\begin{aligned}\begin{bmatrix} \dot{{}^w\omega_w} \\ {}^w\dot{\omega}_{dis,w} \end{bmatrix} &= \begin{bmatrix} \frac{K_t}{R_s\ I_w} \\ 0 \end{bmatrix} v_s - \begin{bmatrix} \frac{K_t\ K_e + B_v\ R_s}{R_s\ I_w}\,{}^w\omega_w - \frac{B_c}{I_w}\mathrm{sign}({}^w\omega_w) + {}^w\omega_{dis,w} \\ 0 \end{bmatrix} \\ &+ \begin{bmatrix} L \\ 0 \end{bmatrix} {}^w\omega_{act,w} + \begin{bmatrix} 0 \\ P \end{bmatrix} {}^w\dot{\omega}_{dis,w} \\ y &= \begin{bmatrix} {}^w\omega_w \\ {}^w\omega_{dis,w} \end{bmatrix} \end{aligned} \tag{8}$$

The unobservability distribution algorithm is used to calculate $\sum_*^P$.

$$\begin{aligned} S_0 &= \bar{P} = \mathrm{span}\left\{ \begin{bmatrix} 0 \\ 1 \end{bmatrix} \right\} \\ S_1 &= \bar{S}_0 + \sum_{i=0}^{1} \left[g_i, \bar{S}_0 \cap \mathrm{Ker}\{\mathrm{d}h\} \right] = \bar{S}_0 \end{aligned} \tag{9}$$

since $\mathrm{Ker}\{\mathrm{d}h\} = [0 \quad 0]^{\mathrm{T}}$. $\sum_*^P (= \bar{S}_2)$ is involutive, contains P and is conditioned invariant, thereby fulfilling the requirements.

$$\begin{aligned} Q_0 &= \left(\sum_*^P \right)^{\perp} \cap \mathrm{span}\{\mathrm{d}h\} = \mathrm{span}\left\{ \begin{bmatrix} 1 \\ 0 \end{bmatrix} \right\} \cap \mathrm{span}\left\{ \begin{bmatrix} 1 \\ 0 \end{bmatrix} \begin{bmatrix} 0 \\ 1 \end{bmatrix} \right\} = \mathrm{span}\left\{ \begin{bmatrix} 1 \\ 0 \end{bmatrix} \right\} \\ Q_1 &= \left(\sum_*^P \right)^{\perp} \cap \left(\sum_{i=0}^{m} L_{g_i} Q_k + \mathrm{span}\{\mathrm{d}h\} \right) = \mathrm{span}\left\{ \begin{bmatrix} 1 \\ 0 \end{bmatrix} \right\} \end{aligned} \tag{10}$$

So the unobservable subspace Δ has to contain $\mathrm{span}\left\{ [0 \quad 1]^{\mathrm{T}} \right\}$ and the disturbance has to be in the unobservable subspace. Using $\Omega \cap \mathrm{span}\{\mathrm{d}h\} = \mathrm{span}\{\mathrm{d}(\Psi_1 \circ h)\}$ to calculate Ψ_1. Since $\Omega \cap \mathrm{span}\{\mathrm{d}h\} = \mathrm{span}\left\{ [1 \quad 0]^{\mathrm{T}} \right\}$, then $\Psi_1 \circ h$ will only contain the ${}^w\omega_w$-state. H_2 is chosen as $[0 \quad 1]$. This results in the following output for the coordinate changed system.

$$y = \begin{bmatrix} {}^w\omega_w \\ {}^w\omega_{dis,w} \end{bmatrix} = \begin{bmatrix} 1 & 0 \\ 0 & 1 \end{bmatrix} \begin{bmatrix} {}^w\omega_w \\ {}^w\omega_{dis,w} \end{bmatrix} \tag{11}$$

Using $\Omega = \mathrm{span}\{\mathrm{d}\psi_1\}$, the H_2 from above and the fact that $\psi_3(x) \in \emptyset$, the state is derived as:

$$\psi(x) = \begin{bmatrix} x_1 \\ x_2 \\ x_3 \end{bmatrix} = \begin{bmatrix} \psi_1(x) \\ H_2 h(x) \\ \psi_3(x) \end{bmatrix} = \begin{bmatrix} {}^w\omega_w \\ {}^w\omega_{dis,w} \end{bmatrix} \tag{12}$$

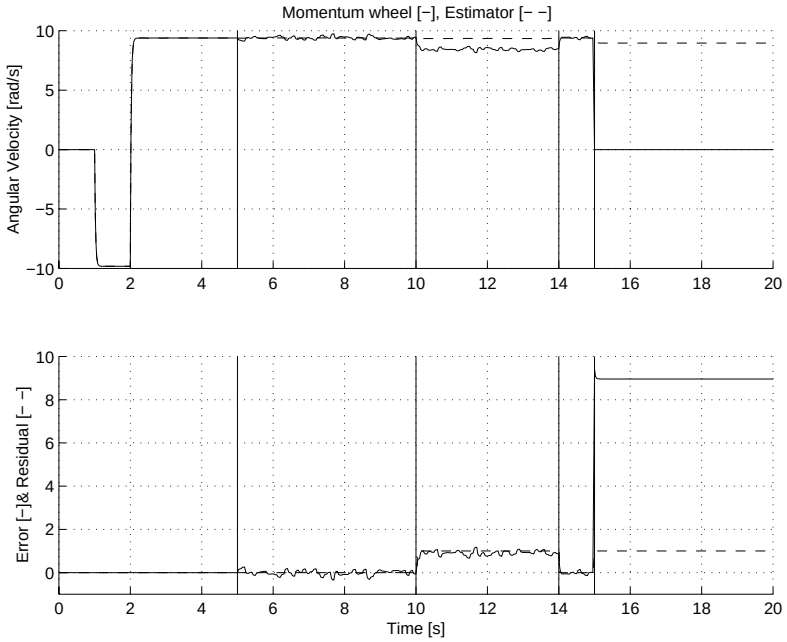

Figure 1. Test of the FDI algorithm.

So if the disturbance is predicted, then it is possible to isolate the actuator fault from the disturbance. This gives the following observer:

$$\begin{aligned} {}^{w}\dot{\omega}_{obs,w} &= \frac{K_t}{R_s\ I_w} v_s - \frac{K_t\ K_e + B_v\ R_s}{R_s\ I_w} {}^{w}\omega_{obs,w} - \frac{B_c}{I_w}\text{sign}({}^{w}\omega_{obs,w}) + {}^{w}\omega_{dis,w} \\ &\quad + K_{obs}({}^{w}\omega_w - {}^{w}\omega_{obs,w}) \\ r &= {}^{w}\omega_{obs,w} - {}^{w}\omega_w \end{aligned} \tag{13}$$

5. SIMULATION TESTS OF THE ALGORITHMS

The simulation test is divided into four subtests. The first subtest examines if the algorithms are sensible to input change. The second subtest investigates if noise under a certain level effects the algorithms. The third and fourth subtest shows the detection times for slow integrating faults (e.g. 10% power loss) and abrupt faults (e.g. shaft breakage).

The results from the tests are identical, so only the results for first algorithm is illustrated in this paper.

Fig. 1 shows the four subtests. The first subtest is in the period 0 to 5 seconds. This subtest shows that the algorithms are not sensitive to voltage changes, which result in variations up to ± 10 rad/s. The second subtest starts after the first, and continues to the end of the test. This subtest shows that noise under a certain level will not effect the fault detection. The third subtest (The period from 10 to 14 seconds) shows that a power loss reduction of 10% is detectable after 0.04 second. The last subtest (From 15 seconds) shows that fast faults are detectable under 0.0001 second.

6. CONCLUSION

The presented method has improved performance and a lower percentage of erroneous fault detections compared to linear and statistical FDI methods. The method can employ a lower threshold for some systems, and

Table 4. Faults geometric FDI cannot isolate.

L	P	$\sum_*^P$
Actuator fault	Sensor fault (Pseudo-actuator fault)	$\text{span}\left\{\begin{bmatrix}0 & 1\end{bmatrix}^{\mathrm{T}}\right\}$
Actuator fault	Disturbance	$\text{span}\left\{\begin{bmatrix}1 & 0\end{bmatrix}^{\mathrm{T}}\begin{bmatrix}0 & 1\end{bmatrix}^{\mathrm{T}}\right\}$
Actuator fault with fault dynamics	Sensor fault with fault dynamics	$\text{span}\left\{\begin{bmatrix}0 & 0 & 1\end{bmatrix}^{\mathrm{T}}\right\}$
Sensor fault with fault dynamics	Actuator fault with fault dynamics	$\text{span}\left\{\begin{bmatrix}1 & 0 & 0\end{bmatrix}^{\mathrm{T}}\begin{bmatrix}0 & 1 & 0\end{bmatrix}^{\mathrm{T}}\right\}$
Actuator fault with fault dynamics	Disturbance with disturbance dynamics	$\text{span}\left\{\begin{bmatrix}1 & 0 & 0\end{bmatrix}^{\mathrm{T}}\begin{bmatrix}0 & 0 & 1\end{bmatrix}^{\mathrm{T}}\right\}$
Disturbance with disturbance dynamics	Actuator fault with with fault dynamics	$\text{span}\left\{\begin{bmatrix}1 & 0 & 0\end{bmatrix}^{\mathrm{T}}\begin{bmatrix}0 & 1 & 0\end{bmatrix}^{\mathrm{T}}\right\}$

consequently the method gains a faster detection time. It further allows the detection of faults of relatively minor influence.

The drawbacks of the method are: the need for a full state description and the fact it is not applicable on all systems. The full state information does however not present a serious problem, since the state description of satellites is well known, leaving only the constants in the actuators and sensors to be determined. The second drawback is a bigger problem and limits the use of the method to some systems, but the first part of the method might still be used to analyse the system.

The system configurations in table 4 are not isolatable, since there is no observable subspace, where $\sum_*^P$ is in the unobservable subspace. With other words there are no output which is not effected by the disturbance and undesired faults.

ACKNOWLEDGEMENTS

The support for this work is by the Danish Research Agency under contract 9902486 “Advanced Control Concepts for Precision Pointing at Small Spacecraft”.

REFERENCES

[1] M. Modarres. *What Every Engineer Should Know About Reliability and Risk Analysis.* Marcel Dekker Inc.:p. 163, 1993.

[2] A. Isidori. *Nonlinear control systems.* Springer-Verlag, 1995.

[3] C. De Persis and A. Isidori. On the observability codistributions of a nonlinear system. *Elsevier*, Systems & Control Letters 40:pp. 297–304, 2000.

[4] C. De Persis and A. Isidori. On the observability codistributions of a nonlinear system. *Elsevier*, Systems & Control Letters 40:pp. 298–299, 2000.

[5] A. Isidori. *Nonlinear control systems.* Springer-Verlag:p. 19, 1995.

[6] C. De Persis and A. Isidori. On the observability codistributions of a nonlinear system. *Elsevier*, Systems & Control Letters 40:pp. 299–300, 2000.

[7] Gene F. Franklin et al. *Feedback Control of Dynamic Systems.* Addison-Wesley Publishing Company, 3 edition:p. 49, 1994.